PLASMA SHEATH CHARACTERIZATION FOR TELEMETRY IN HYPERSONIC FLIGHT

Ryan P. Starkey and Mark J. Lewis
Department of Aerospace Engineering
University of Maryland, College Park, MD 20742

Charles H. Jones
412 TW/ENTI
Edwards AFB, California

ABSTRACT

During certain hypersonic flight regimes, shock heating of air creates a plasma sheath resulting in telemetry attenuation or blackout. The severity of the signal attenuation is dependent on vehicle configuration, flight trajectory, and transmission frequency. This phenomenon is investigated with a focus placed on the nonequilibrium plasma sheath properties (electron concentration, plasma frequency, collision frequency, and temperature) for a range of flight conditions and vehicle design considerations. Trajectory and transmission frequency requirements for air-breathing hypersonic vehicle design are then addressed, with comparisons made to both shuttle orbiter and RAM-C II reentry flights.

KEY WORDS

Hypersonic plasma telemetry, plasma sheath, radio blackout alleviation, aerodynamic shaping, nonequilibrium plasma.

INTRODUCTION

For the realm of hypersonics (characterized by velocities greater than five times the speed of sound), ground testing is only possible to a certain point after which flight testing becomes necessary. The test and evaluation (T&E) of operational air-breathing hypersonic cruise vehicles will be a challenge. One of the major challenges will be the difficulty of radio frequency telemetry through a plasma field. During certain hypersonic regimes, the plasma field generated around a vehicle can cause signal attenuation or complete communication blackout. Standard T&E procedures require real-time telemetry monitoring at all times, primarily for flight safety reasons. Without real-time monitoring it is extremely difficult to make quick decisions on when to abort a flight. This safety issue becomes significant if the vehicle is capable of sustained hypersonic flight. (Note that Mach 10 flight allows travel to anywhere in the world in about 2 hours; a strong military reason for developing a vehicle capable of such velocities.)

A secondary reason for desiring the ability of real-time telemetry is for catastrophe analysis. Data collected milliseconds prior to a catastrophe could be critical in determining the cause, especially at hypersonic velocities (greater than about 1.5 km/s). In this case, real-time data telemetry could be absolutely critical since the velocities and altitudes involved imply that it is unlikely that onboard recorders would survive a crash (or be found if they do survive). These points are further reinforced by the recent shuttle Columbia tragedy; telemetry was lost prior to vehicle disintegration and little data was available on the recorder once it was recovered. A tertiary reason for real-time monitoring is flight point validation. This is mostly a cost issue, but during normal envelope expansion, it is faster and cheaper to be able to verify a test point during flight and proceed to the next test point without having to land and takeoff in between.

There are three dominant mission scenarios for which telemetry through a plasma sheath is a concern: 1) an air-breathing hypersonic cruise vehicle, 2) an access to space vehicle, and 3) a ballistic missile. Although these missions seem fundamentally different, the general physics involved in the electromagnetic wave/plasma sheath interaction are the same. The access to space vehicle and ballistic missile are designed to leave and subsequently reenter the earth's atmosphere. These types of vehicles could be traveling at velocities up to Mach 26 (about 8 km/s). An air-breathing access to a space vehicle would spend much more of its flight within earth's atmosphere than a ballistic missile, and would likely be in a communication blackout for a significant amount of time. The air-breathing hypersonic cruise vehicle, which remains within the earth's atmosphere to provide oxidizer for its engine(s), also has the added concern that for a majority of its flight profile, the vehicle could be enveloped within a plasma sheath. The cruise vehicle can be envisioned as a missile, a weapon delivery platform, or a reconnaissance vehicle, and thus be traveling at any hypersonic Mach number. Current Air Force T&E concerns are to develop the ability to test air-breathing hypersonic cruise and access to space vehicles before the need arises. The trajectories that these types of vehicles might take are shown in figure 1.

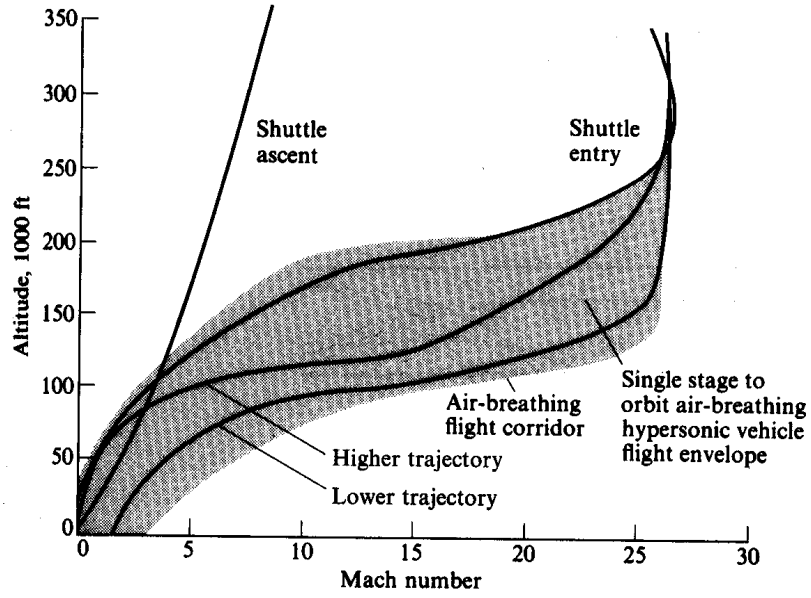

Figure 1: Flight corridor for various access-to-space type vehicles (from Anderson[13]).

Telemetry through plasma layers becomes essential when acknowledging the fact that most air-breathing hypersonic vehicle concepts are unmanned aerial vehicles (UAVs), including missiles, reconnaissance and weapon delivery platforms, and test versions of access to space vehicles. Public acceptance of a UAV in sustained hypersonic flight under autonomous control, especially if it is a weapon or capable of delivering a weapon, would be unlikely. As such, if current hypersonic vehicle designs were to become operational they could not be tested in the United States (or elsewhere) for the reasons cited previously unless continuous telemetry could be guaranteed.

HYPERSONIC FLOWFIELD

The ability to communicate through a plasma sheath (the layer of ionized gas between the shock wave and the vehicle surface) remains a critical area of research in hypersonic flight.[1-5] The plasma is an electrically charged gas consisting of neutral and ionized species as well as free electrons and is assumed to be neutrally charged for this study (equal number of ions and free electrons). Although it is known that the mechanism of plasma generation is through the shock heating of the air above the molecular dissociation and ionization temperature, the mechanism of how to control or modify the plasma is not sufficiently understood.

During the communication blackout portion of the flight the plasma is generally characterized by electron concentrations on the order of 10^{14} to 10^{20} electrons/m^3, depending on the configuration, trajectory, and location within the shock layer. It is the free electrons that attenuate or absorb the electromagnetic wave, especially when the transmission frequency is near to or less than the plasma frequency.[6] The signal attenuation problem can also be further complicated by the presence of ablation products in the flowfield.

A rudimentary understanding of the blackout mechanism is generated by numerically integrating the conservation equations for mass, momentum, energy, and species for flow through inviscid, one-dimensional shock waves for a range of flight conditions. An 11 species (N_2, O_2, N, O, NO, N_2^+, O_2^+, N^+, O^+, and e), 20 reaction mechanism[11,12] is used to model the nonequilibrium flow across normal shocks, as well as shocks generated by 20, 30, and 40 degree wedges. The oblique shocks are assumed to be the frozen values for simplicity.

Since hypersonic vehicles that have been flown until now have been reentry vehicles, they will be used as test points. Two such vehicles are the space shuttle orbiter, as shown in figure 2, and the Radio Attenuation Measurements C-II (RAM-C II) flight test vehicle[14,15] as shown in figure 3. The shuttle orbiter represents a blunt body type reentry (although not as blunt as an Apollo capsule) and the RAM-C II is a slender type vehicle, which may be more indicative of the leading-edge shape of an air-breathing hypersonic vehicle. Air-breathing hypersonic cruise and access to space vehicles currently being researched are designed with sharp leading edges to minimize losses due to drag[7], as shown by the missile in figure 4.

Regardless of the vehicle configuration, at some point and scale on the vehicle, a normal bow shock will exist (assuming a realistic amount of leading-edge blunting for heat transfer considerations), which will taper off to a weaker oblique shock. Depending on the configuration and angle of attack, some or all of the flow ionized by the leading edge will pass by the transmitter/receiver (generally located as far aft as

possible). The more slender the body and shallower the angle of attack generally will result in lower ionization rates, thinner plasma sheath, and a much more benign flowfield for telemetry considerations. However, shallow angles of attack result in all of the stagnation flow passing over the vehicle and a thinner plasma sheath may indicate a relative increase in electron concentration.

Figure 2: Space Shuttle Orbiter

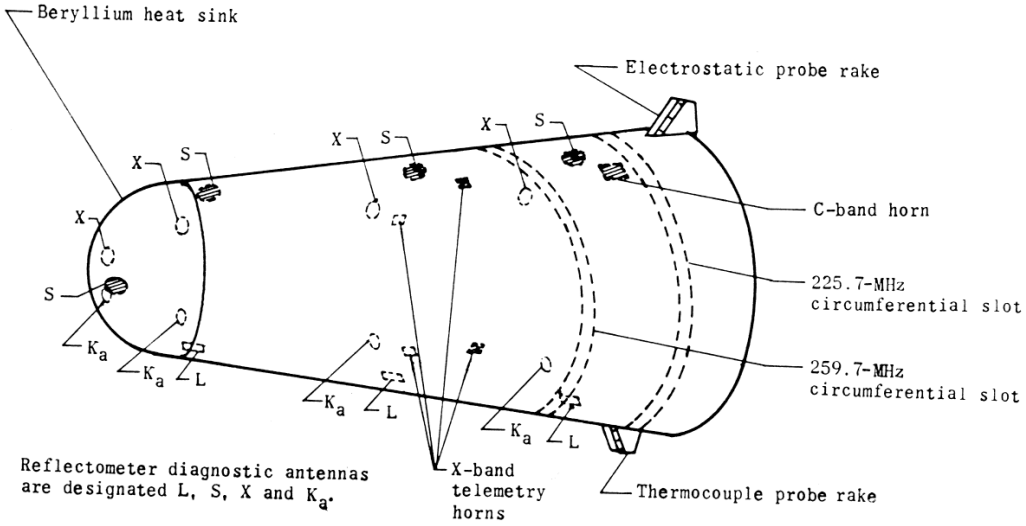

Figure 3: Radio Attenuation Measurements C-II flight test vehicle[16]

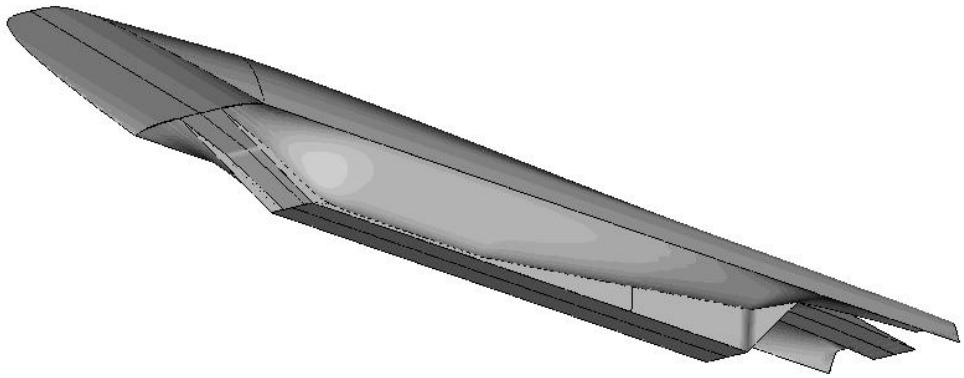

Figure 4: Air-Breathing Hypersonic Missile Concept[7]

ELECTROMAGNETIC WAVE INTERACTION WITH PLASMA SHEATH

With a general understanding of the type of flowfield a vehicle might encounter, a broader understanding of what causes the problem of communication blackout must be addressed. This will aid in determining solutions to possible alleviation of the signal attenuation associated with the interaction between an electromagnetic wave and the plasma sheath.

The plasma frequency ω_p is the natural frequency at which the free electron oscillates in the presence of a plasma[9]

$$\omega_p = \sqrt{\frac{n_e q_e^2}{\varepsilon_0 m_e}} \approx 56.416\sqrt{n_e} \tag{1}$$

where:

n_e = electron density [m^{-3}]
q_e = electron charge constant [-1.602×10^{-19} C]
ε_0 = free space dielectric constant [$10^7/(4\pi c^2)$ F/m]
m_e = electron mass constant [9.107×10^{-31} kg]

For one-dimensional plane-wave solutions of electromagnetic wave propagation into a plasma, it can be shown that $\mathbf{E} = \mathbf{E_0} \exp[(\alpha_p - i\beta_p)x]$ with the plasma attenuation coefficient α_p and phase coefficient β_p given by[2,10]

$$\alpha_p = k_0 \left[\frac{\sqrt{\varepsilon_r^2 + \varepsilon_i^2} - \varepsilon_r}{2} \right]^{1/2} \tag{2}$$

and

$$\beta_p = k_0 \left[\frac{\sqrt{\varepsilon_r^2 + \varepsilon_i^2} + \varepsilon_r}{2} \right]^{1/2} \tag{3}$$

where:

k_0 = ω/c is the free space wave number [m^{-1}]
ω = electromagnetic wave frequency [s^{-1}]
c = speed of light [3×10^8 m/s]

The real and imaginary parts of the effective dielectric coefficient are given by

$$\varepsilon_r = 1 - \frac{\omega_p^2}{\omega^2 + \nu^2} \tag{4}$$

and

$$\varepsilon_i = \frac{\omega_p^2 (\nu/\omega)}{\omega^2 + \nu^2} \tag{5}$$

respectively, where ν is the electron collision frequency [s^{-1}].

Using equations 2 and 3, the special case of an electromagnetic wave propagating in a collisionless plasma (i.e., $\nu=0$) can be considered. In this instance, both the attenuation coefficient α_p and the imaginary part of effective dielectric coefficient ε_i are identically equal to zero. Therefore, for a wave frequency ω greater than the plasma frequency ω_p, the wave propagates without attenuation. When ω is less than ω_p, the electric field is given by an exponentially decaying wave. If $\omega = \omega_p$ then ε_r is also zero and the electromagnetic wave is totally reflected at the surface and does not propagate into the plasma.

The simple distinctions which were made previously for a lossless plasma do not hold when the electron collision frequency becomes significant. For this lossy plasma case (i.e., $\nu\neq0$), the value of ε_i exists at all frequencies. Therefore, the plane wave will propagate with attenuation for all cases. Generally, as the wave frequency increases, the attenuation coefficient α_p decreases, prompting a desire for large values of ω. Also, in the instance where the electron collision frequency ν becomes greater than the wave frequency ω, the attenuation coefficient α_p decreases thereby reducing attenuation (although not as significantly as for cases where $\omega > \omega_p$). The plasma attenuation and phase constants are plotted versus normalized frequency for various normalized collision frequencies in figure 5.

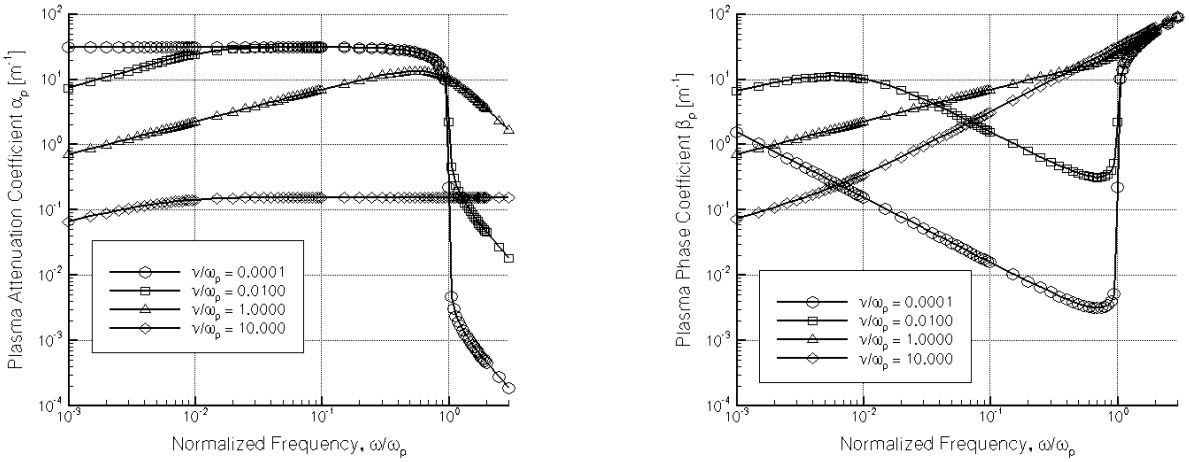

a) Plasma attenuation coefficient

b) Plasma phase coefficient

Figure 5: Plasma Attenuation and Phase Coefficients versus Normalized Transmission Frequency for a Range of Normalized Collision Frequencies.[6]

COMPARISON WITH BLACKOUT FLIGHT DATA

Using the methodologies defined previously for solving the steady, inviscid, nonequilibrium plasma flow through shock waves to determine the electron concentration and attenuation constant (equation 2), the space shuttle orbiter and RAM C-II flight tests were examined. Figure 6 shows the space shuttle

blackout trajectory while figure 7 shows the RAM C-II blackout trajectory. The plasma attenuation coefficient $\alpha_p = 1$ for nonequilibrium flow through shock waves are plotted as contour lines for various wedge angles using the peak electron concentration. The right side of each contour line is the blackout area and the left side is where telemetry can take place.

It should be noted that errors in the calculations are evident at both high and low altitudes where the peak electron concentrations will likely never be reached due to velocity and pressure effects, respectively. At higher altitudes, the mean free path will become sufficiently large where continuum modeling of the flow is inaccurate and a Direct Simulation Monte Carlo (DSMC) methodology should be used. Also, the collision frequency was set equal to the electron production rate, which is an underestimation of ν since each collision does not necessarily result in an ionization or recombination reaction taking place.

Space Shuttle Orbiter

The space shuttle orbiter ascent and descent trajectories along with the known blackout start and termination points are shown in figure 6. The shuttle orbiter transmits at a frequency $f = 2.1064$ GHz and has an angle of attack of about 40 degrees throughout its 16 minute blackout. During its reentry the orbiter uses a large number of 'S-turns' to slowly dissipate energy. It is likely that the unsteady effects from the turning in combination with the high altitude velocity effects mentioned above contribute to the shuttle exhibiting the effective attenuation coefficient equivalent to a 30-degree wedge during the deceleration from Mach 26 to Mach 18. After this point the effective attenuation coefficient steadily increases from a 30-degree wedge equivalent (at Mach 18) to a flat plate equivalent (at Mach 9), where the shuttle emerges from blackout. It is through this second part of the reentry that the shuttle transitions from a slender body approximation to a blunt body, flat plate flow field. This indicates that the stagnation flow region on the shuttle is exhibiting greater influence on the telemetry mechanism, most likely due to boundary layer, and frozen flow effects.

Radio Attenuation Measurements C-II Flight Test Vehicle

Being a much more slender body, the RAM C-II flight test vehicle will have a much more viscous dominated plasma sheath, with higher electron concentrations than calculated here using Euler equations. Strong shock boundary layer interactions at the leading edge will produce larger shock angles than predicted by inviscid theory, resulting in higher electron concentrations. Also, since the beryllium heat sink nose cap was ejected at about 56 km (near its melting point), Teflon ablation products in the flowfield increase the electron concentration over the theories presented here. Finally, since the vehicle was only 1.3 m long with a 0.3 m nose diameter and the total wind angle was oscillating between 2 and 6 degrees (both pitch and yaw wobble) the flowfield was unsteady and wake flow likely contributed to signal attenuation. Since the effects of ambipolar diffusion are not included, errors are expected[17] in the computed electron concentration above 70 km. The RAM C-II vehicle transmitted at a frequency $f =$ 259.7 MHz.

The effective attenuation coefficient for the RAM C-II vehicle varied from about 30 degrees at the onset of blackout, dropped below 20 degrees for a short while, and was about 22 degrees at the end of blackout. Overall, the RAM C-II vehicle behaved much more like a simple slender body, accounting for the errors as previously mentioned, than the shuttle orbiter. It should be noted that errors are expected

when using a two-dimensional wedge approximation for an axisymmetric configuration. Conical flow solutions would result in larger cone angles (than wedge angles) for a similar attenuation coefficient.

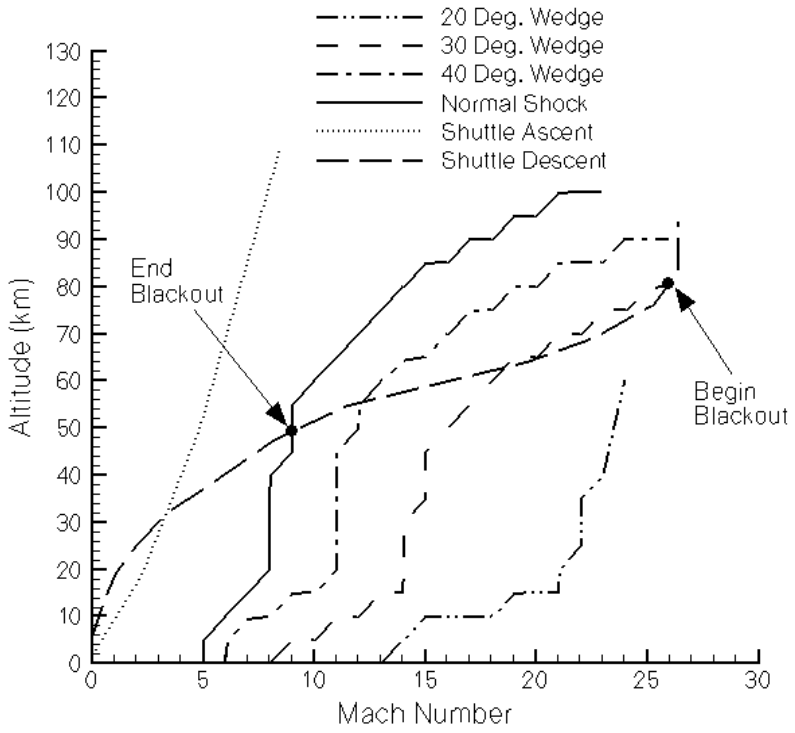

Figure 6: Blackout Points Along the Reentry Trajectory for the Space Shuttle Orbiter Along with Plasma Attenuation Coefficient Unity Lines for Various Wedge Angles

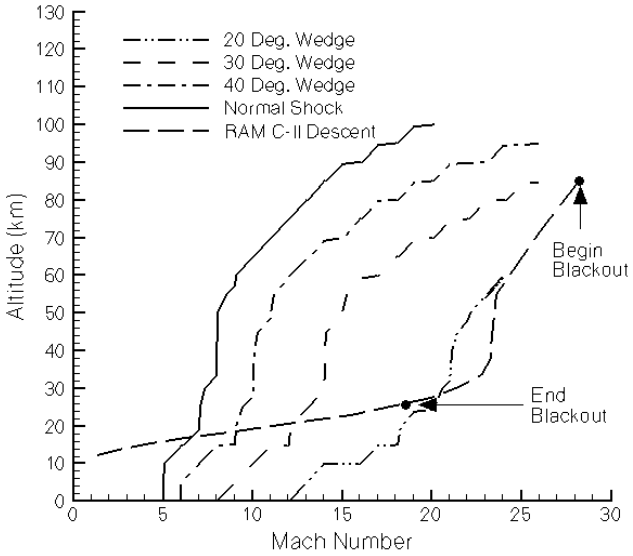

Figure 7: Blackout Points Along the Reentry Trajectory[19] for the RAM C-II Flight Test Vehicle Along with Plasma Attenuation Coefficient Unity Lines for Various Wedge Angles

AIR-BREATHING HYPERSONIC FLIGHT TESTING

With a little bit of insight into the complications of blackout prediction at various points in a trajectory, as well as configurational effects, an investigation into the blackout phenomena for air-breathing configurations can be done. Figure 8 shows the calculated values for plasma frequency as a function of trajectory position for four different wedge angles. The range of plasma frequencies of interest on the figures are ω_p = 1E9 s^{-1} to 1E11 s^{-1} which translate to transmissions frequencies of f = 0.16 GHz to 16.0 GHz. The air-breathing flight corridor from figure 1 has been overlaid for reference. Air-breathing hypersonic vehicle configurations will be significantly different than either of the two extremes presented previously, but sources of error will be similar, such as shock boundary layer interaction effects (making slender bodies appear much blunter), frozen flow, and ambipolar diffusion. As expected, the trends show that the more slender the body, the higher the altitudes and Mach numbers are before blackout occurs for frequencies in the S, C, X, and Ku-bands.

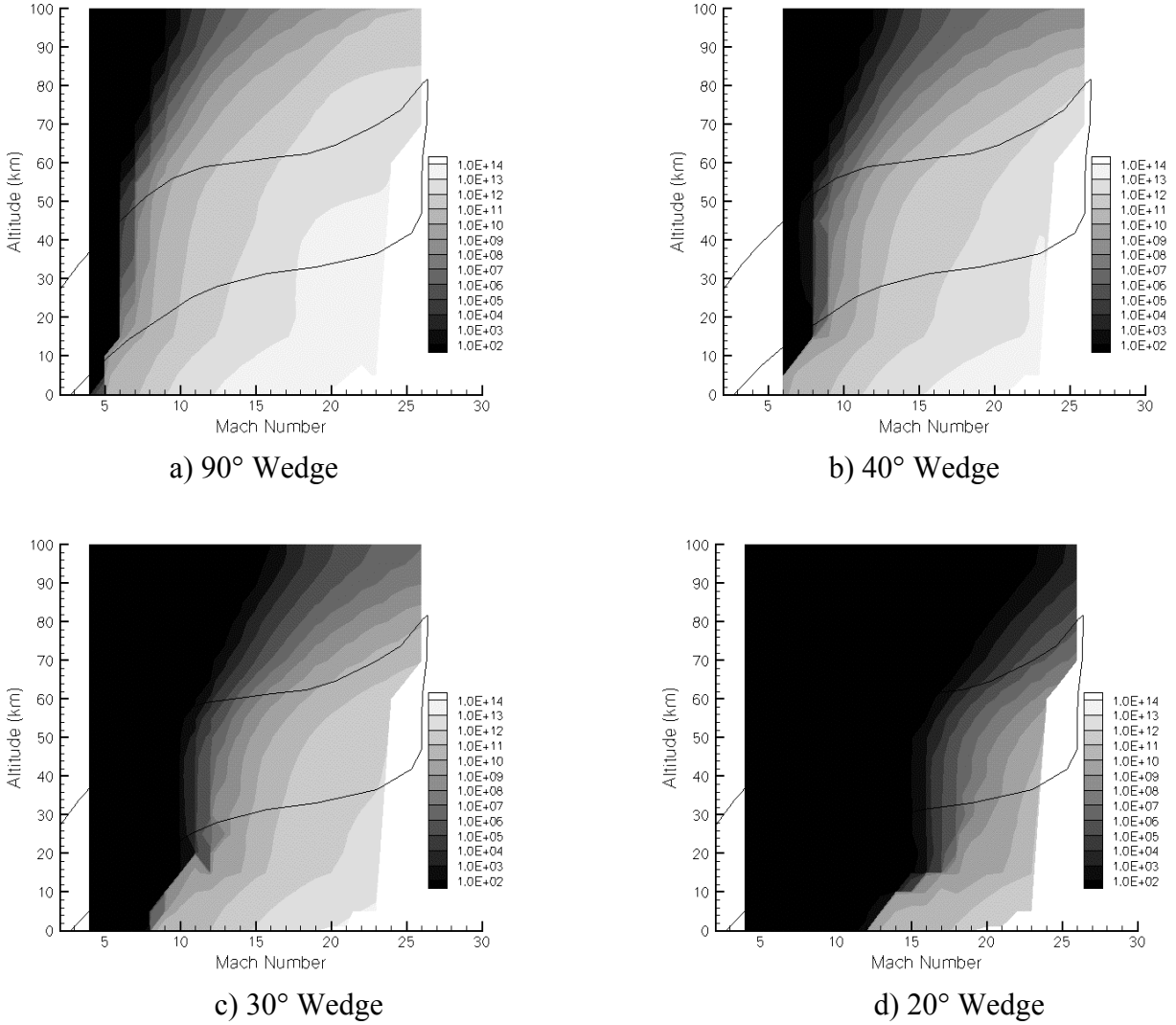

a) 90° Wedge

b) 40° Wedge

c) 30° Wedge

d) 20° Wedge

Figure 8: Plots of Mach Number verses Altitude with Plasma Frequency Contours for four Different Wedge Angles. Solid Lines Indicate the Air-Breathing Flight Corridor from Figure 1.

CONCLUSIONS

The exercise of approximating a complex configuration along a three-dimensional trajectory with an unsteady flowfield using a single point shock comparison calculated using an inviscid, steady, nonequilibrium plasma chemistry approach has been detailed. Comparisons to flight data for both the space shuttle orbiter and RAM C-II reentries have been done to understand the nature of the approximations. The approximation was then applied to the air-breathing hypersonic vehicle flight regime resulting in approximate bounds for blackout frequencies for simple body approximations.

ACKNOWLEDGMENTS

This research is supported by the Center for Hypersonic Education and Research at the University of Maryland under technical monitor of Dr. Charles Jones of the Air Force Flight Test Center at Edwards Air Force Base, the support of whom is greatly appreciated.

REFERENCES

1. Dirsa, E., "The Telemetry and Communication Problem of Re-Entrant Space Vehicles," Proceedings of the Institute for Radio Engineers, Volume 48, April 1960, Pages 703-713.
2. Rybak, J., and Churchill, R., "Progress in Reentry Communications," IEEE Transactions on Aerospace and Electronic Systems, Volume 7, September 1971, Pages 879-894.
3. Nusca, M., "Electromagnetic Attenuation in Plasmas Generated by Atmospheric Flight," *Journal of Thermophysics and Heat Transfer*, Vol. 11, No. 2, Apr-June 1997, pp. 304-306.
4. Steinkopf, M., "Mission Accomplished – Final Report on the Atmospheric Reentry Demonstrator," http://esapub.esrin.esa.it/onstation/onstation5/ard5.pdf, March 2001.
5. Belov, I. F., Gorelov, V. A., Kireev, A. Y., Korolev, A. S., and Stepanov, E. A., "Investigation of Remote Antenna Assembly for Radio Communication with Reentry Vehicle," *Journal of Spacecraft and Rockets*, Vol. 38, No. 2, Mar-Apr 2001, pp. 249-256.
6. Starkey, R. P., and Lewis, M. J., "Aerodynamic Shaping Effects on Re-Entry Plasma Sheath Telemetry Blackout," AIAA 2002-5267, October 2002.
7. Starkey, R. P., "Hypersonic Air-Breathing Missile Designs Within External Box Constraints," Ph.D. Dissertation, University of Maryland, College Park, Maryland, 2000.
8. Cambel, A. B., Plasma Physics and Magnetofluidmechanics, Mc-Graw Hill Book Company, Inc., New York, 1963.
9. Krall, N. A., and Trivelpiece, A. W., Principles of Plasma Physics, Mc-Graw Hill Book Company, Inc., New York, 1973.
10. Friel, P. J., and Rosenbaum, B., "Propagation of Electromagnetic Waves Through Reentry-Induced Plasmas," Advances in the Astronautical Sciences (Jacobs, H., ed.), Vol. 11, pp. 141-255, American Astronautical Society, 1963.
11. Gnoffo, P. A., Gupta, R. N., and Shinn, J. L., "Conservation Equations and Physical Models for Hypersonic Air Flows in Thermal and Chemical Nonequilibrium," NASA TP-2867, 1989.
12. Gupta, R. N., Yos, J. M., Thompson, R. A., and Lee, K., "A Review of Reaction Rates and Thermodynamic and Transport Properties for an 11-Species Air Model for Chemical and Thermal Nonequilibrium Calculations to 30000 K," *NASA RP-1232*, 1990.

13. Anderson, J. D., Hypersonic and High Temperature Gas Dynamics, Mc-Graw Hill Book Company Inc., New York, 1989.
14. Akey, N. D., "Overview of RAM Reentry Measurements Program," The Entry Plasma Sheath and its Effects on Space Vehicle Electromagnetic Systems, Vol. 1, pp. 19-31, NASA SP-252, 1970.
15. Huber, P. W., and Sims, T. E., "The Entry-Communications Problem," Astronautics and Aeronautics, Vol. 2, Oct 1964, pp. 30-40.
16. Park, Chul, Nonequilibrium Hypersonic Aerothermodynamics, John Wiley & Sons, Inc., 1990.
17. Grantham, W., "Reentry Plasma Measurements Using a Four-Frequency Reflectometer," The Entry Plasma Sheath and its Effects on Space Vehicle Electromagnetic Systems, Vol. 1, pp. 65-108, NASA SP-252, 1970.